HHS Public Access

Author manuscript

Magn Reson Med. Author manuscript; available in PMC 2021 May 17.

Published in final edited form as:

Magn Reson Med. 2019 February ; 81(2): 765–772. doi:10.1002/mrm.27441.

Calibration of methylene-referenced lipid-dissolved xenon frequency for absolute MR temperature measurements

Michael A. Antonacci[a,b], **Le Zhang**[b,c], **Simone Degan**[d], **Detlev Erdmann**[e], **Rosa T. Branca**[a,b,*]

[a]Department of Physics and Astronomy, University of North Carolina at Chapel Hill, USA

[b]Biomedical Research Imaging Center, University of North Carolina at Chapel Hill, USA

[c]Department of Applied Physical Sciences, University of North Carolina at Chapel Hill, USA

[d]Center for Molecular and Biomolecular Imaging, Department of Radiology and Dermatology, Duke University, Durham, NC, USA

[e]Division of Plastic, Reconstructive, Maxillofacial and Oral Surgery, Duke University Medical Center, USA

Abstract

Purpose—Absolute MR temperature measurements are currently difficult because they require pre-calibration specific for tissue types and conditions. Reference of the lipid-dissolved ^{129}Xe resonance frequency to temperature-insensitive methylene protons (rLDX) has been proposed to remove the effect of macro- and microscopic susceptibility gradients to obtain absolute temperature information. The scope of this work is to evaluate the rLDX chemical shift (CS) dependence on lipid composition to estimate the accuracy of absolute temperature measurements in lipids.

Methods—Neat triglycerides, vegetable oils, and samples of freshly-excised human and rodent adipose tissue (AT) are prepared under ^{129}Xe atmosphere and studied using high-resolution NMR. The rLDX CS is measured as a function of temperature. ^{1}H spectra are also acquired and the consistency of methylene-referenced water proton and rLDX CS values are compared in human AT.

Results—Although rLDX CS shows a dependence on lipid composition, in human and rodent AT samples the rLDX shows consistent CS values with a similar temperature dependence (−0.2058±0.0010) ppm/°C + (200.15±0.03) ppm, enabling absolute temperature measurements with an accuracy of 0.3°C. Methylene-referenced water CS values present variations of up to 4°C, even under well-controlled conditions.

Conclusions—The rLDX can be used to obtain accurate absolute temperature measurements in AT, opening new opportunities for hyperpolarized ^{129}Xe MR to measure tissue absolute temperature.

*Correspondence to: Rosa Tamara Branca, Ph.D., Department of Physics and Astronomy, University of North Carolina at Chapel Hill, Chapel Hill, NC 27599. rtbranca@unc.edu.

Keywords

chemical shift; xenon spectroscopy; brown adipose tissue; magnetic resonance spectroscopy; absolute thermometry

INTRODUCTION

Temperature, one of the most fundamental physical properties of matter, is extremely hard to measure non-invasively in vivo. The temperature dependence of the resonance frequency of water protons (PRF) is linear and nearly independent with respect to tissue type(1). As such, by measuring the PRF with respect to that of a temperature-insensitive resonance, one could in principle extract absolute temperature information(2). Aside from the brain, in other regions of the body, precise absolute temperature measurements are difficult. While the temperature-insensitive resonance of methylene protons might seem like a good candidate for a stable reference, magnetic susceptibility gradients generated at water-fat interfaces, coupled with the relatively strong temperature dependence of the magnetic susceptibility of fat(3), lead to temperature inaccuracy of several degrees Celsius(4–6). As a result, it is not surprising that very different temperature calibrations of the water-methylene resonance frequency have been reported over the years(7–9).

Recently, it was shown that the resonance frequency of xenon dissolved in adipose tissue (AT), also called lipid-dissolved ^{129}Xe (LDX), had a strong linear temperature dependence (−0.2 ppm/°C) in the physiologically-relevant temperature range of 25–45°C(6,10) and higher (11). It was also suggested that, by referencing the LDX to that of the temperature-insensitive methylene protons in a volume in which xenon dissolves, absolute temperature information could be obtained(6). Absolute temperature measurements could be valuable not only for calibration of more conventional MR thermometry methods used to monitor temperature during hyperthermia treatment of lipid-containing tumors(12), but also for the detection of thermogenic activity of brown adipose tissue (BAT), a tissue specialized in heat production that is currently being considered as a good target for the treatment of obesity and diabetes(13). Considering that the LDX signal is the primary signal observed in vivo in hyperpolarized ^{129}Xe spectra of rodent(10) and human(14) BAT, measurements of absolute temperature by LDX could provide a direct window to BAT thermogenic activity which, so far, can only be detected indirectly via infrared thermography (15,16). However, because previous studies have reported differences in the chemical shift (CS) of xenon dissolved in different kinds of oils (11,17), and considering that BAT temperature needs to be measured with an accuracy better than 1°C, the scope of this work was to investigate whether the methylene-referenced LDX (rLDX) signal had a dependence on lipid composition that could affect the accuracy with which absolute temperature measurements can be made.

METHODS

Sample preparation

Samples of neat triglycerides (triolein (18:1), trielaidin (18:1T), trilinolein (18:2), trilinoelaidin (18:2T), tripalmitolein (16:1), and tripalmitelaidin (16:1T) (number of

carbons:number of double carbon bonds, where T indicates *trans* isomers)), were obtained from NuChek Prep, Inc, Elysian, MN, while neat corn and olive oils were obtained from Sigma-Aldrich and whole kernel, unrefined coconut oil from Dr. Bronner's (www.drbronner.com). Rat and mouse AT samples were excised from the animals immediately following euthanasia. All animal studies were performed under protocols approved by the Institutional Animal Care and Use Committee at the University of North Carolina at Chapel Hill. Human AT samples were obtained after de-identification from 6 patients undergoing abdominoplasty/panniculectomy surgery. The surgically removed tissue was rapidly transported to a sterile hood for dissection of the AT using forceps and surgical scissors. The AT was then transported on ice to the facility housing the NMR spectrometer and samples were immediately prepared.

For NMR measurements, all samples were placed in a high-pressure NMR tube (Daedalus Innovations, LLC, Aston, Pennsylvania, USA) connected to a home-built vacuum pump system. Samples were frozen in liquid nitrogen, evacuated with a rotary pump, and thawed. This process was repeated 3 times to ensure that all oxygen was removed from the sample. Each sample was then equilibrated for 24 hours with >86% isotopically enriched ^{129}Xe gas to a pressure of about 1 atm in order to avoid Xe-Xe chemical shift contributions(6).

High-resolution NMR spectroscopy

Prepared oil, triglyceride and tissue samples were all studied by high-resolution NMR on a 500 MHz spectrometer (Varian NMR Systems, Palo Alto, California, USA). Samples were equilibrated for about 1 hour in the spectrometer at temperatures of approximately 25°C, 30°C, 35°C, and 40°C. Temperatures were maintained by a variable temperature controller and calibrated with an accuracy of 0.1°C at the beginning of each spectroscopy experiment using a 100% methanol temperature standard.

All samples were manually shimmed using up to the 7th order z shim and 4th order x and y shims. Proton spectra were acquired before and after ^{129}Xe spectra in order to confirm consistent conditions throughout the ^{129}Xe acquisition. Proton spectra were acquired with a center frequency (CF) of 499.7828127 MHz, repetition time (TR) of 6 s, spectral width (SW) of 5998 Hz, 11996 points, 16 averages, and 6° flip angle. The proton TR was chosen to ensure full relaxation of triglyceride protons, since the proton spectra were also used to measure fat saturation, as described below. ^{1}H T_1 and T_2 measurements were also performed on the triglyceride peaks of interest in one human AT sample at 37°C and the data were processed on the spectrometer using VNMRJ software (Varian). ^{129}Xe spectra were acquired with a CF of 138.2672519 MHz, TR=26 s, SW=60015 Hz, 120030 points, 36 averages, and 46° flip angle.

Measurement of Triglyceride Saturation by ^{1}H NMR

For all samples, lipid saturation was measured as described in Refs (18,19). Briefly, the total unsaturated fatty acid (FA) content was calculated using the integrated areas of the spectral peaks of the allylic protons (A, at 2.03 ppm) and protons α to COO (B, at 2.25 ppm; αCOO). Unsaturated FA fraction was determined by

$$f_{unsat} = \frac{1}{2}\frac{A}{B} \quad (1)$$

where the factor of 1/2 accounts for there being twice as many allylic protons than αCOO protons in each FA chain. Then, the fraction of saturated FAs was calculated from

$$f_{sat} = 1 - f_{unsat}\,. \quad (2)$$

Spectral Analysis and Estimation of Uncertainties

Proton spectra were processed by first applying an automatic phase correction method implemented in MATLAB (MathWorks, Natick, MA, USA)(20). Both phased proton and magnitude ^{129}Xe spectra were fit in MATLAB using a non-linear, iterative algorithm to either Lorentzian or Voigt line shape models that incorporated linear or quadratic baseline correction(21). Uncertainties in the methylene peak position were estimated from the fit results. Uncertainties in the measurement of triglyceride and neat oil saturation by ^{1}H NMR were calculated as the standard deviation of the measured saturation values at all temperatures. The uncertainties in saturation for human samples were calculated by adding in quadrature the maximum variation in pure triglyceride samples to the standard deviation of measured saturation values for the human samples at each temperature.

Temperature measurements by rLDX CS were performed as described in previous work(6,22). Briefly, the water frequency, assumed to be 3.5 ppm downfield from the measured methylene frequency, was scaled by 3.6152950216 (i.e. by the ratio of the gyromagnetic ratios of ^{1}H and ^{129}Xe) to find a fictitious 0 ppm reference for the rLDX CS.

In order to accurately calibrate the temperature dependence of the rLDX CS, each CS measurement was plotted as a function of the sample temperature calibrated on the NMR spectrometer as described above. The final data was fitted to a linear model by the method described in Ref (23) in order to appropriately weight the experimental uncertainties in temperature and CS at each data point. The uncertainty of the final temperature calibration curve was calculated by first rearranging the rLDX CS versus temperature fit to solve for temperature, and then propagating, in quadrature, the standard errors in the calibrated temperature coefficient, CS offset, and typical experimental CS uncertainty of 0.02 ppm in the rLDX spectrum.

RESULTS

Lipid saturation by ^{1}H spectroscopy

T_1 and T_2 values for the allylic protons were measured to be 0.629±0.007 s and 0.176±0.005 s, and for the αCOO protons were 0.672±0.021 s and 0.178±0.004 s, respectively. No T_1 or T_2 corrections were needed for quantitative analysis as observed T_2^* values were less than 0.035 s. Saturation values for all samples measured are shown in Table 1. Variations in measured saturation uncertainties in the human AT samples are the result of variations in the achievable field homogeneity, which led to varying degrees of overlap between the adjacent allylic and αCOO peaks.

^{129}Xe chemical shift dependence on lipid saturation in neat triglycerides and oils

Figure 1 shows plots of the rLDX CS versus temperature in neat triglyceride and oil samples. Although all of the triglycerides analyzed were unsaturated, substantial variation in the CS offset is observed with varying hydrocarbon chain length, number of double bonds, and isomer. In the neat vegetable oil samples, the CS offset seems also to vary with the degree of lipid saturation. Based on the measurements in pure unsaturated triglycerides, the CS offset most likely depends on the composition of the unsaturated triglycerides in each of these oils (see the Discussion section below).

Absolute rLDX temperature calibrations in human adipose tissue

Figure 2 shows plots of the rLDX CS versus temperature in AT samples collected from 6 different subjects, along with results from mouse and rat AT samples. Within the physiologically-relevant temperature range, the rLDX CS is linear and the model best fit for the human data is (−0.2058±0.0010) ppm/°C + (200.15±0.03) ppm when accounting for the individual measurement uncertainties, as described above. Rearranging and propagating the model standard errors, the temperature measurement by rLDX CS is accurate to within 0.3°C.

Comparison with ^{1}H–methylene absolute thermometry

Lastly, we analyzed the accuracy of temperature estimation performed by using the previously reported relation between the ^{1}H-methylene frequency separation and temperature(7,8) that have also been used in vivo to directly measure absolute temperature in human ATs. Table 2 presents temperature measurements performed on human AT sample 6 at 5 different temperatures using the ^{1}H-methylene CS separation method in the high-resolution NMR spectrometer. Interestingly, even under well-controlled conditions (thermally equilibrated and relatively homogeneous AT sample), the measured absolute temperature can vary from the calibrated sample temperature by over 4°C, depending on which ^{1}H-methylene CS separation calibration is used.

DISCUSSION

The rLDX CS studies of triglycerides and neat oils clearly show that the rLDX CS and its temperature dependence varies with the type of oil/triglyceride analyzed. The temperature dependence for triglycerides is close to −0.20 ppm/°C, whereas for neat oils it is slightly higher and close to −0.21 ppm/°C. Although the oils examined here have a wide range of lipid saturations, with high saturation producing lower rLDX CS values, a bare dependence of rLDX CS on the degree of lipid saturation does not seem to be sufficient to explain the observed variations in the CS offset. We therefore examined the dependence of the rLDX CS on other factors that varied between samples, including density, fraction of medium-chained fatty acids (6–12 C atoms), fraction of double carbon bonds (FDCB), and average hydrocarbon chain length (AHCL), as shown in Figure 3. Using literature values for the composition of the neat oils (24,25) and human AT(26), FDCB was calculated by

$$FDCB = \frac{\sum_i f_i D_i}{\sum_i f_i B_i}, \quad (3)$$

where f_i is the fraction of component i in the sample, D_i is the number of double carbon bonds in component i, and B_i is the total number of bonds in the hydrocarbon chain of component i. Similarly, AHCL was calculated by

$$AHCL = \frac{\sum_i f_i A_i}{\sum_i f_i}, \quad (4)$$

where A_i is the number of the carbon atoms in the hydrocarbon chain, and the denominator serves as a normalization factor for the human AT composition, of which only 94% of the components were reported (26). Surprisingly, neither density nor fraction of medium-chained fatty acids show a clear correlation with rLDX CS. On the other hand, both FDCB and AHCL seem to correlate with rLDX CS (Fig 3d,e). This dependence is not surprising and consistent with the dependence on the methylene/methyl ratio previously found by Lim et al (27) for the CS of xenon dissolved in n-alkanes at constant temperature. This dependence, as later described by Yuan et al (28), does not arise from a higher contribution of CH_2 than CH_3 to the xenon CS, but to the fact that these measurements were made at a constant temperature rather than at constant thermodynamic state(28,29). The observed increase in CS with the number of double bonds is likely due to the through-space intermolecular deshielding effect of the carbon-carbon double bond. Of course, a double bond also produces a kink in the molecule and an increase in the “void size” sampled by xenon that, in turn, should lead to a decrease in xenon CS. These two effects (increase in void size and increase in deshielding effect in the presence of a double bond) drive the xenon CS in opposite directions. However, the increase in CS due to the deshielding effect of a carbon-carbon double bond seems to be greater than the decrease in CS due to the increase in void size, as shown by comparison of CS values obtained in *cis* and *trans* configurations of triglycerides. For example, as can be seen in Figure 1a, the difference in CS is more remarkable between the triolein and trilinolein, which have comparable void sizes but a different number of carbon-carbon double bonds, than between the triolein and trielaidin, which have different void sizes but the same number of double bonds. Of course, to quantitatively separate each of these contributions to the xenon CS, molecular dynamics simulations should be performed.

Despite the variation in rLDX CS among the triglycerides and neat oil samples found here, the rLDX CS seems to be consistent across all human AT samples, reflecting the similar composition and saturation of human AT at the molecular level (26). Furthermore, even the rodent AT samples agree reasonably well with the human results, despite that the composition of rodent AT is expected to vary from that of humans, primarily because of differences in diet. Interestingly, this consistency is similar to the consistency found for the temperature dependence of T_1 and T_2 of methylene and methyl protons (30) in bovine fat, porcine fat, olive oil and mayonnaise, highlighting the high similarity of these samples at the molecular level. In light of these results, it is reasonable to assume that even if a larger number of human AT samples were to be analyzed, no significant differences in rLDX CS

would be observed. This suggests that the rLDX CS can indeed be used to obtain absolute temperature information in vivo with an accuracy of 0.3°C when using the rLDX temperature calibration obtained here. Of course, in vivo, a subject's motion and broadening of the resonance frequency lines could decrease temperature accuracy; however, local shimming procedures performed on the methylene protons, coupled with a sequential acquisition of the ^{1}H and ^{129}Xe spectra, can minimize these effects. On the other hand, any effect due to shimming conditions or tissue microscopic structure is completely eliminated by referencing the LDX frequency to that of the nearby methylene protons in which xenon dissolves. This opens up the opportunity to directly measure absolute temperature in adipose tissues like BAT, where the major dissolved-phase peak observed during cold exposure after inhalation of a single 600 mL bag of hyperpolarized xenon originates from xenon dissolved in the lipids of BAT (14).

Since the linear dependence of the rLDX CS, which arises from the linear decrease of solvent density with increasing temperature, is expected to exist for a much wider temperature range(11), application of rLDX thermometry for temperature calibration of current proton MR thermometry methods in lipid-rich tumors could be envisioned. As demonstrated here, microscopic susceptibility gradients generated at water-fat interfaces often degrade the accuracy with which absolute temperature can be measured using methylene-referenced PRF. In these spectra, the water and methylene peaks were well-resolved and well-fit at each temperature, and the peak centroids were determined with negligible uncertainty. Even so, the ^{1}H-methylene CS separation temperature calibrations previously reported led to an absolute temperature error up to 4°C. While specific applications may exist where a 4°C error can be acceptable, such as monitoring of tissue temperature during thermal ablation treatment of cancers, for others, such as the quantification of BAT thermogenesis in humans, a higher degree of accuracy is necessary.

CONCLUSIONS

In this work, we analyzed the dependence of the rLDX frequency for different oil and human AT samples. Although the rLDX frequency seems to depend on FDCB and AHCL, the small variation in composition that exists across human AT does not significantly affect the rLDX CS. By using the rLDX temperature calibration found in these studies, absolute human AT temperature can, under optimal conditions, be obtained directly from the rLDX frequency with an accuracy of 0.3°C, as compared to several °C for the prior ^{1}H methylene temperature calibration method.

Acknowledgments

This work was supported by NIH grant fund R01 DK108231.

References

1. Rieke V, Butts Pauly K. MR thermometry. J. Magn. Reson. Imaging. 2008; 27:376–390. DOI: 10.1002/jmri.21265 [PubMed: 18219673]
2. Cady EB, D'Souza PC, Penrice J, Lorek A. The Estimation of Local Brain Temperature by in Vivo 1H Magnetic Resonance Spectroscopy. Magn. Reson. Med. 1995; 33:862–867. DOI: 10.1002/mrm.1910330620 [PubMed: 7651127]

3. Sprinkhuizen SM, Bakker CJG, Ippel JH, Boelens R, Viergever MA, Bartels LW. Temperature dependence of the magnetic volume susceptibility of human breast fat tissue: an NMR study. Magn. Reson. Mater. Physics, Biol. Med. 2012; 25:33–39. DOI: 10.1007/s10334-011-0250-2
4. Baron P, Deckers R, Bouwman JG, Bakker CJG, de Greef M, Viergever MA, Moonen CTW, Bartels LW. Influence of water and fat heterogeneity on fat-referenced MR thermometry. Magn. Reson. Med. 2016; 75:1187–1197. DOI: 10.1002/mrm.25727 [PubMed: 25940426]
5. Sprinkhuizen SM, Konings MK, Van Der Bom MJ, Viergever MA, Bakker CJG, Bartels LW. Temperature-induced tissue susceptibility changes lead to significant temperature errors in PRFS-based MR thermometry during thermal interventions. Magn. Reson. Med. 2010; 64:1360–1372. DOI: 10.1002/mrm.22531 [PubMed: 20648685]
6. Zhang L, Burant A, McCallister A, Zhao V, Koshlap KM, Degan S, Antonacci M, Branca RT. Accurate MR thermometry by hyperpolarized 129Xe. Magn. Reson. Med. 2017; 78:1070–1079. DOI: 10.1002/mrm.26506 [PubMed: 27759913]
7. Kuroda K, Mulkern RV, Oshio K, Panych LP, Nakai T, Moriya T, Okuda S, Hynynen K, Joles FA. Temperature mapping using the water proton chemical shift: Self-referenced method with echo-planar spectroscopic imaging. Magn. Reson. Med. 2000; 43:220–225. DOI: 10.1002/(SICI)1522-2594(200002)43:2<220::AID-MRM8>3.0.CO;2-9 [PubMed: 10680685]
8. Hernando D, Sharma SD, Kramer H, Reeder SB. On the confounding effect of temperature on chemical shift-encoded fat quantification. Magn. Reson. Med. 2014; 72:464–470. DOI: 10.1002/mrm.24951 [PubMed: 24123362]
9. Koskensalo K, Raiko J, Saari T, Saunavaara V, Eskola O, Nuutila P, Saunavaara J, Parkkola R, Virtanen KA. Human Brown Adipose Tissue Temperature and Fat Fraction Are Related to Its Metabolic Activity. J. Clin. Endocrinol. Metab. 2017; 102:1200–1207. DOI: 10.1210/jc.2016-3086 [PubMed: 28323929]
10. Branca RT, He T, Zhang L, Floyd CS, Freeman M, White C, Burant A. Detection of brown adipose tissue and thermogenic activity in mice by hyperpolarized xenon MRI. Proc. Natl. Acad. Sci. U. S. A. 2014; 111:18001–18006. DOI: 10.1073/pnas.1403697111 [PubMed: 25453088]
11. Venkatesh A, Kacher DK, Kuroda K, Balamore D, Jolesz F, Albert M. Temperature measurement using the 129Xe chemical shift. Proc. Int. Soc. Magn. Reson. Med. 2001; 9:2194.
12. Germain D, Chevallier P, Laurent A, Saint-Jalmes H. MR monitoring of tumour thermal therapy. Magma Magn. Reson. Mater. Physics, Biol. Med. 2001; 13:47–59. DOI: 10.1007/BF02668650
13. Nedergaard J, Cannon B. The Changed Metabolic World with Human Brown Adipose Tissue: Therapeutic Visions. Cell Metab. 2010; 11:268–272. DOI: 10.1016/j.cmet.2010.03.007 [PubMed: 20374959]
14. Branca, RT, Zhang, L, Burant, A, Katz, L, McCallister, A. Proceedings of the International Society of Magnetic Resonance in Medicine. Singapore: 2016. Detection of human brown adipose tissue by MRI with hyperpolarized Xe-129 gas and validation by FDG-PET/MRI; 1054
15. Cypess AM, Haft CR, Laughlin MR, Hu HH. Brown Fat in Humans: Consensus Points and Experimental Guidelines. Cell Metab. 2014; 20:408–415. DOI: 10.1016/j.cmet.2014.07.025 [PubMed: 25185947]
16. Lee P, Ho KKY, Lee P, Greenfield JR, Ho KKY, Greenfield JR. Hot fat in a cool man: infrared thermography and brown adipose tissue. Diabetes, Obes. Metab. 2011; 13:92–93. DOI: 10.1111/j.1463-1326.2010.01318.x [PubMed: 21114609]
17. Miller KW, Reot NV, Uiterkampt AJMS, Stengle DP, Stengle TR, Williamson KL. Xenon NMR : Chemical shifts of a general anesthetic in common solvents, proteins, and membranes. Proc. Natl. Acad. Sci. 1981; 78:4946–4949. [PubMed: 6946442]
18. Ren J, Dimitrov I, Sherry AD, Malloy CR. Composition of adipose tissue and marrow fat in humans by 1 H NMR at 7 Tesla. J. Lipid Res. 2008; 49:2055–2062. DOI: 10.1194/jlr.D800010-JLR200 [PubMed: 18509197]
19. Strobel K, van den Hoff J, Pietzsch J. Localized proton magnetic resonance spectroscopy of lipids in adipose tissue at high spatial resolution in mice in vivo. J. Lipid Res. 2008; 49:473–480. DOI: 10.1194/jlr.D700024-JLR200 [PubMed: 18024705]

20. Bao Q, Feng J, Chen L, Chen F, Liu Z, Jiang B, Liu C. A robust automatic phase correction method for signal dense spectra. J. Magn. Reson. 2013; 234:82–89. DOI: 10.1016/j.jmr.2013.06.012 [PubMed: 23851024]
21. O'Haver T. Command-line peak fitter for time-series signals. 2016
22. Antonacci MA, Zhang L, Burant A, McCallister D, Branca RT. Simple and robust referencing system enables identification of dissolved-phase xenon spectral frequencies. Magn. Reson. Med. 2017; doi: 10.1002/mrm.27042
23. York D, Evensen NM, Martínez ML, De Basabe Delgado J. Unified equations for the slope, intercept, and standard errors of the best straight line. Am. J. Phys. 2004; 72:367–375. DOI: 10.1119/1.1632486
24. Hovorková P, Laloučková K, Skřivanová E. Determination of in vitro antibacterial activity of plant oils containing medium-chain fatty acids against Gram-positive pathogenic and gut commensal bacteria. Czech J. Anim. Sci. 2018; 63:119–125. DOI: 10.17221/70/2017-CJAS
25. Cui Y, Hao P, Liu B, Meng X. Effect of traditional Chinese cooking methods on fatty acid profiles of vegetable oils. Food Chem. 2017; 233:77–84. DOI: 10.1016/j.foodchem.2017.04.084 [PubMed: 28530614]
26. Hodson L, Skeaff CM, Fielding BA. Fatty acid composition of adipose tissue and blood in humans and its use as a biomarker of dietary intake. Prog. Lipid Res. 2008; 47:348–380. DOI: 10.1016/j.plipres.2008.03.003 [PubMed: 18435934]
27. Lim YH, King AD. NMR chemical shifts of xenon-129 dissolved in liquid n-alkanes and their mixtures. J. Phys. Chem. 1993; 97:12173–12177. DOI: 10.1021/j100149a012
28. Yuan H, Murad S, Jameson CJ, Olson JD. Molecular Dynamics Simulations of Xe Chemical Shifts and Solubility in n-Alkanes. J. Phys. Chem. C. 2007; 111:15771–15783. DOI: 10.1021/jp0735233
29. Jameson CJ, Sears DN, Murad S. Molecular dynamics averaging of Xe chemical shifts in liquids. J. Chem. Phys. 2004; 121:9581–9592. DOI: 10.1063/1.1807817 [PubMed: 15538880]
30. Kuroda K, Iwabuchi T, Obara M, Honda M, Saito K, Imai Y. Temperature dependence of relaxation times in proton components of fatty acids. Magn. Reson. Med. 2011; 10:177–83. DOI: 10.2463/mrms.10.177

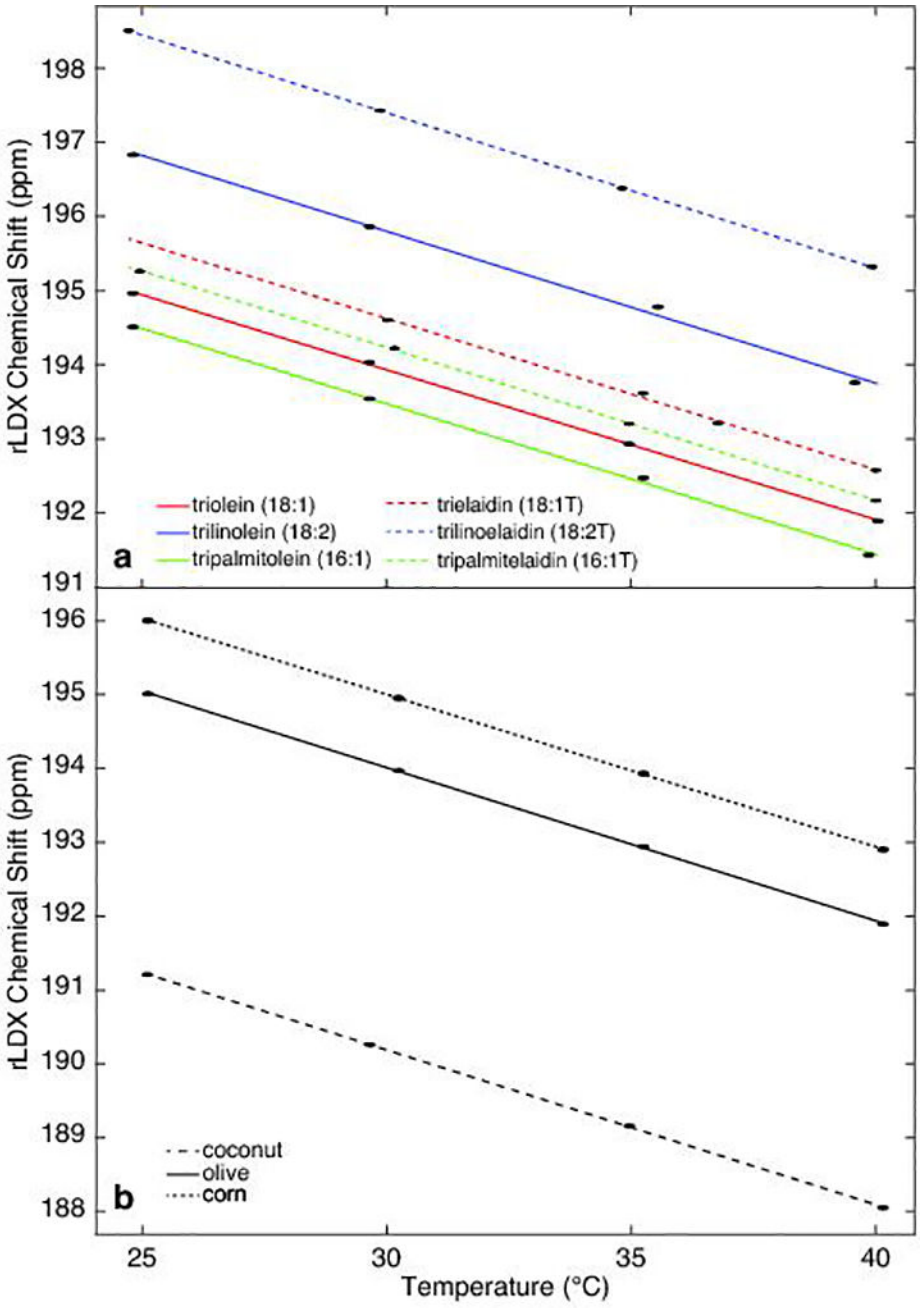

FIG. 1.

Plots of rLDX chemical shift versus sample temperature for neat (a) triglycerides and (b) vegetable oils. Experimental uncertainties for each measurement are indicated by elliptical regions around each point. Best fits for rLDX CS curves for 18:1, 18:2, and 16:1 samples are (−0.2021±0.0025) ppm/°C+(199.99±0.08) ppm, (−0.2045±0.0025) ppm/°C+(201.93±0.08) ppm, and (−0.2031±0.0025) ppm/°C+(199.57±0.08) ppm, respectively. Best fits for 18:1T, 18:2T, and 16:1T are (−0.2042±0.0042) ppm/°C+(200.76±0.15) ppm, (−0.2101±0.0027) ppm/°C+(203.71±0.09) ppm, and (−0.2066±0.0027) ppm/°C+(200.44±0.09) ppm, respectively. Best fits for coconut, olive, and corn oils are (−0.2097±0.0026) ppm/°C

+(196.49±0.08) ppm, (−0.2073±0.0026) ppm/°C+(200.24±0.09) ppm, and (−0.2059±0.0032) ppm/°C+(201.18±0.11) ppm, respectively.

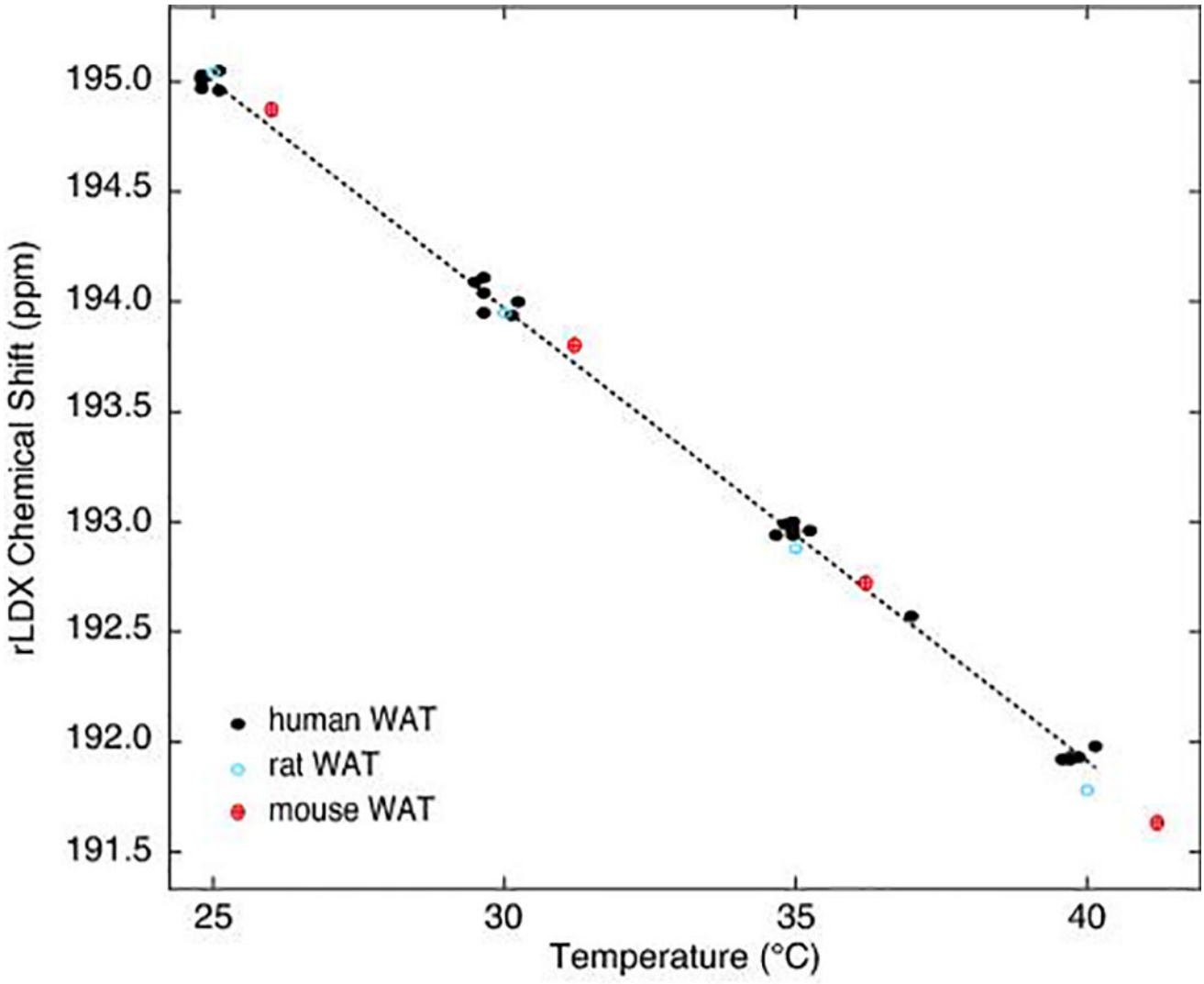

FIG. 2.

Plot of rLDX chemical shift versus temperature for all human AT samples, and comparison with rat and mouse AT samples. Experimental uncertainties for each measurement are represented by elliptical shaded regions. The fitted curve takes into account the experimental uncertainties at each point in both temperature and rLDX chemical shift resulting in a temperature dependence of (−0.2058±0.0010) ppm/°C + (200.15±0.03) ppm for human WAT. The absolute temperature calibration uncertainty, calculated by propagating the standard error in the temperature coefficient and chemical shift offset, and assuming an experimental rLDX CS uncertainty of 0.02 ppm, is less than 0.3 °C within the physiologically-relevant temperature range. The rat and mouse rLDX CS temperature dependences are (−0.2170±0.0026) ppm/°C + (200.47±0.09) ppm and (−0.2135±0.0033) ppm/°C + (200.44±0.11) ppm, respectively.

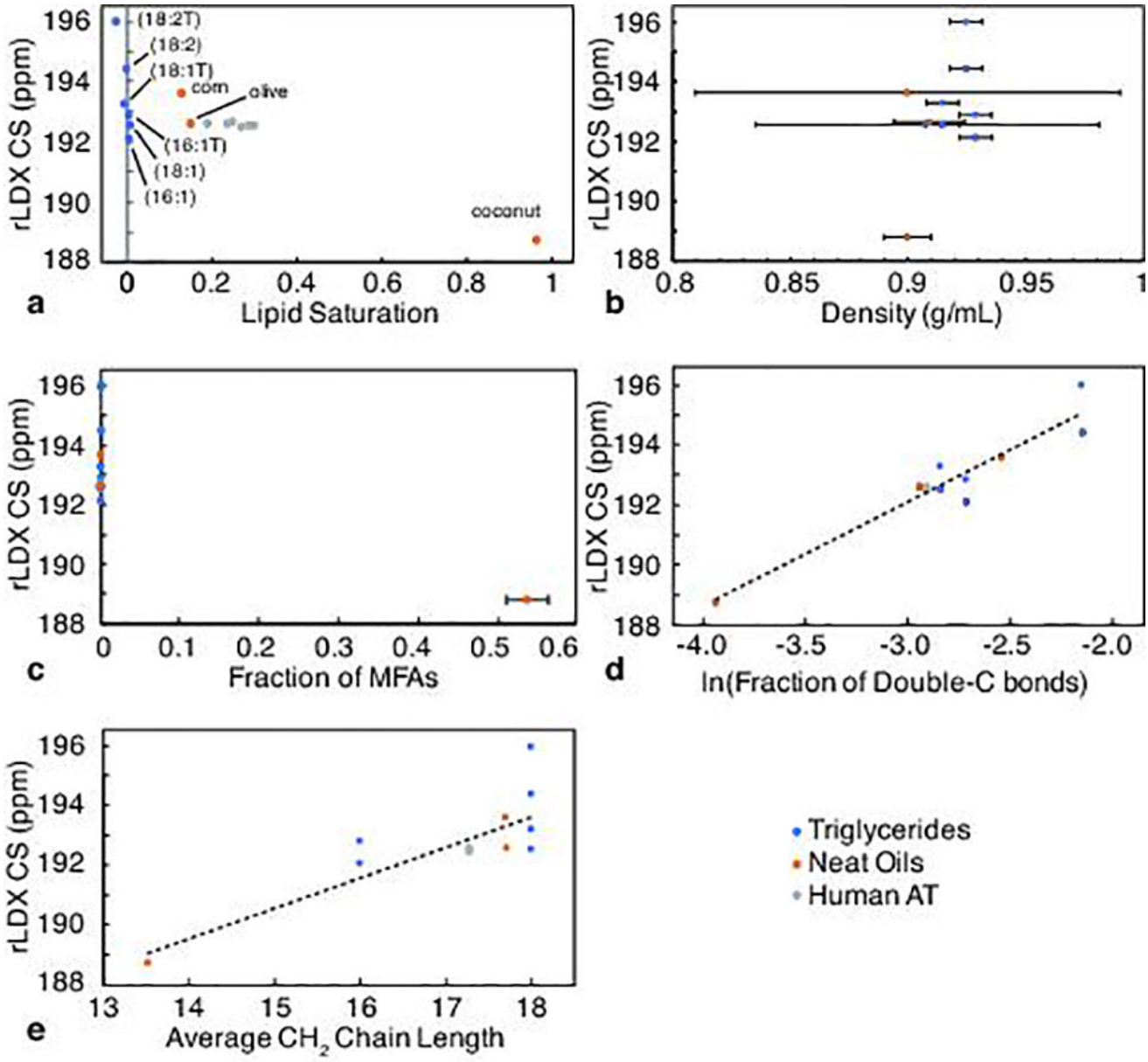

FIG. 3.

Plots of rLDX chemical shift at 37°C versus **(a)** lipid saturation, (**b**) density, (**c**) fraction of medium-chain fatty acids, **(d)** ln of the fraction of double-carbon bonds (FDCB), and **(e)** average hydrocarbon chain length (AHCL). FDCB and AHCL are calculated as described above. Fit lines for **(d)** and **(e)** are 3.470ln(FDCB)+202.48 ppm and 1.017(AHCL)+175.31 ppm, with R^2 values of 0.906 and 0.654, respectively. Error bars are omitted from **(a)** for clarity; values are given in Table 1.

Table 1

Fraction of saturated fatty acids in each sample as measured by ^{1}H NMR and corresponding rLDX frequency at 37°C.

Sample	Known fraction of saturated fatty acids	Measured fraction of saturated fatty acids[a]	Uncertainty[b]	rLDX frequency at 37°C (ppm)[c]
18:1	0.00	0.010	0.015	192.51±0.02
18:2	0.00	−0.005	0.013	194.37±0.02
16:1	0.00	0.007	0.012	192.06±0.02
18:1T	0.00	−0.005	0.021	193.20±0.02
18:2T	0.00	−0.023	0.007	195.94±0.02
16:1T	0.00	0.007	0.024	192.80±0.02
Olive Oil	---	0.152	0.004	192.57±0.02
Corn Oil	---	0.129	0.009	193.57±0.03
Coconut Oil	---	0.966	0.006	188.73±0.02
Human AT 1	---	0.29	0.10	192.51±0.02
Human AT 2	---	0.25	0.09	192.60±0.02
Human AT 3	---	0.27	0.06	192.45±0.02
Human AT 4	---	0.24	0.02	192.54±0.03
Human AT 5	---	0.30	0.03	192.50±0.02
Human AT 6	---	0.19	0.09	192.56±0.02

[a] These values represent the mean of individual measurements made at each temperature.

[b] Uncertainties for neat oils and triglycerides are given as the standard deviation of the individual measurements made at each temperature. Uncertainties for human AT samples are calculated as described in the Methods section above.

[c] Values interpolated using the linear fits to each sample's data only.

Table 2

Absolute temperature measurement values as obtained in human AT sample 6 by using the ^{1}H-methylene chemical shift-temperature calibrations previously reported in the literature.

Sample temperature (±0.1°C)	^{1}H-CH_2 chemical shift separation (ppm)	Temperature (°C, Kuroda, et al (7))	Temperature (°C, Hernando, et al (8))	Temperature (°C, rLDX method)
25.1	3.445	28.5	27.9	24.8±0.2
30.2	3.370	34.1	34.8	29.9±0.2
35.2	3.319	37.9	39.5	34.9±0.3
37.0	3.338	36.4	37.8	36.8±0.3
39.9	3.280	40.7	43.1	39.9±0.3